Available online at www.sciencedirect.com

ScienceDirect

Mendeleev Commun., 2023, **33**, 135–137

Mendeleev Communications

XAS study of muratite-based ceramics and crystalline film of ThO_2

Andrei E. Putkov,*[a,b] Yury A. Teterin,[a,b] Alexander L. Trigub,[b] Sergey V. Yudintsev,[c,d] Olga I. Stefanovskaya,[d] Kirill E. Ivanov,[b] Stepan N. Kalmykov[a] and Vladimir G. Petrov[a]

[a] *Department of Chemistry, M. V. Lomonosov Moscow State University, 119991 Moscow, Russian Federation. E-mail: andrei.putkov@mail.ru*
[b] *National Research Center 'Kurchatov Institute', 123182 Moscow, Russian Federation*
[c] *Institute of Geology of Ore Deposits, Petrography, Mineralogy and Geochemistry, 119017 Moscow, Russian Federation*
[d] *A. N. Frumkin Institute of Physical Chemistry and Electrochemistry, Russian Academy of Sciences, 119071 Moscow, Russian Federation*

DOI: 10.1016/j.mencom.2023.01.043

The local environment of thorium in muratite ceramics (Al,Ca,Ti,Mn,Fe,Zr,Th)O_x and ThO_2(001) crystalline film on Si(100) substrate as a reference was explored by X-ray absorption spectroscopy (XAS) for the first time. It was found that Th^{4+} is located in the center of a cube formed by 8 oxygen atoms [*r*(Th–O) = 2.37 ± 0.03 Å] in muratite ceramics and ThO_2 film. The Th^{4+} second coordination sphere [*r*(Th–M) ≈ 3.5 Å] in muratite is represented by 3*d* metals: titanium, iron or manganese.

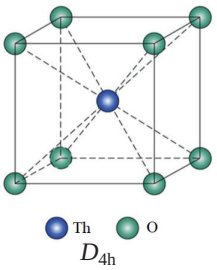

Keywords: EXAFS spectroscopy, muratite-based ceramic, thorium dioxide, crystal film, disposal of nuclear waste.

Actinide-containing high-level waste (HLW) management is one of the most critical problems of the nuclear power technology. The HLW is the long-term hazard since it contains long-lived highly toxic and active actinides. Currently the only method of HLW isolation from biosphere brought to the industrial stage is its vitrification.[1] Glasses are metastable formations and will crystallize with time, which can increase the leaching of radionuclides. So, a search for crystal mineral-like matrices for reliable retention of long-lived radionuclides is currently underway.[2–4] Titanate zirconate ceramics consisting of phases of polysomatic pyrochlore–muratite series with fluorite-like structure are among the most promising matrices.[5] These phases are formed by alternating pyrochlore and muratite blocks. The rate of actinides leaching is one of the most important matrix characteristics. It depends on the position of atoms in the structure, which, in turn, is determined by the valence state and the size of the cation.[6] Actinides cations in various oxidation states can be included in certain phases of ceramic matrices with different retention capacity when interacting with groundwater. Th^{4+} is often considered as an analogue of U^{4+}, Np^{4+}, and Pu^{4+}, at least from the crystallographic viewpoint.

In this work, the EXAFS study of the structure of the Th^{4+} immediate environment in muratite ceramics has been carried out for the first time. The sample was synthesized by melting the mixture composed of 5 wt% Al_2O_3, 10 wt% CaO, 50 wt% TiO_2, 10 wt% MnO_2, 5 wt% Fe_2O_3, 10 wt% ZrO_2 and 10 wt% ThO_2 for 0.5 h in an electric furnace in glass–carbon crucibles at 1500 ºC followed by cooling of furnace to 1300 ºC and crystallization of the melt. The phases in the sample (Figure 1, Table 1) were identified by X-ray diffraction (XRD, Empyrian X-ray powder diffractometer, Cu radiation, 40 kV, 35 mA, Ni filter), scanning electron microscopy [SEM, JSM-5610LV equipped with X-Max 80 energy dispersive spectrometer (SEM/EDX)],[7] and X-ray photoelectron spectroscopy (XPS, Kratos Axis Ultra DLD, AlKα radiation with quantum energy of 1486.7 eV, X-ray tube power 150 W, 20 ºC, 1.3×10^{-7} Pa).[8] A more detailed analysis of phase and chemical composition of the sample is given elsewhere.[7]

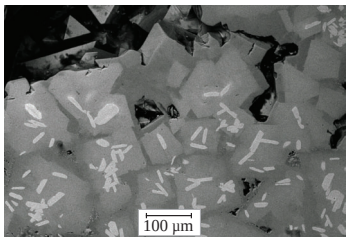

Figure 1 SEM image of the ceramics. Light elongated crystals are zirconolite, grey and dark grains are muratite, black spaces are pores.

The structure of muratite contains pyrochlore-like lattice blocks with fluorite structure similar to that in ThO_2, a = 4.9 Å.[5] For correct interpretation of EXAFS structure of Th-containing ceramics, the ThO_2(001) film on Si(100) substrate (hereinafter ThO_2 film)† was used as a reference. XAS spectra of ThO_2 film

† A ThO_2 crystal film with (001) surface orientation on a Si(100) substrate of 9 × 9 × 2 mm^3 in size was prepared by reactive magnetron sputtering using the Omicron setup at JRC Karlsruhe (Germany). Before film deposition, the substrate was cleaned with ethanol, then it was heated at ~600 °C and $p(O_2) = 2 \times 10^{-6}$ mbar for 40–60 min. A thorium metal target was used as a thorium source, argon was used as a sputtering gas at $p(Ar) = 5.9 \times 10^{-4}$ mbar, and oxygen was used as a reactive gas at $p(O_2) = 7 \times 10^{-6}$ mbar. The temperature of the silicon substrate was maintained close to 600 °C. The film was sputtered for 60 min under conditions that should ensure a film thickness of 140–360 nm. A more detailed information about the ThO_2 crystal film is given elsewhere.[9]

Table 1 Elemental composition of phases (wt%, total 100 wt% for each phase).[a]

Phase	Al	Ca	Ti	Mn	Fe	Zr	Th	O
Zirconolite[b]	0.8	7.5	23.5	3.0	1.1	23.0	10.8	30.3
Zirconolite	0.9	7.1	24.5	3.5	1.3	19.6	12.8	30.3
Zirconolite	1.3	7.2	23.3	2.7	0.6	23.0	11.6	30.3
Murataite[c] (g)	2.5	7.6	30.9	6.9	2.1	7.8	9.4	32.8
Murataite (g)	2.0	7.8	29.2	6.8	1.9	10.0	10.2	32.1
Murataite (g)	1.9	7.4	28.8	6.6	1.9	9.1	12.7	31.6
Murataite (d)	4.6	7.0	33.0	8.2	4.5	2.6	5.2	34.9
Murataite (d)	4.8	7.1	31.8	7.8	4.4	3.0	6.6	34.5
Murataite (d)	4.7	6.4	32.8	8.7	4.8	2.0	5.9	34.7

[a] SEM/EDX data, error of determination 10%, detection limit 0.3–0.5 wt%, g – grey, d – dark (see Figure 1). [b] Card 26324 (Inorganic Crystal Structure Database). [c] Cards 01-086-0888 and 00-036-0138 (International Centre for Diffraction Database).

and muratiate ceramics together with Th immediate environment in ThO_2 are shown in Figure 2.

EXAFS spectrum of Th L_{III}-edge of ThO_2 film and its Fourier transform modulus are presented in Figure 3(*a*),(*b*). The first coordination sphere of Th^{4+} contains 8 oxygen atoms, the interatomic distance *r*(Th–O) is 2.41 ± 0.01 Å, the second and the third coordination spheres are formed by 12 Th and 24 O atoms with interatomic distances 3.98 ± 0.01 and 4.65 ± 0.02 Å, respectively (Table 2). These results agree with the reference data for thorium dioxide.[10]

The EXAFS spectrum of Th L_{III}-edge of muratiate-based ceramic and its Fourier transform modulus are presented in Figure 3(*c*),(*d*). The EXAFS results show that the Th^{4+} first coordination sphere in the ceramic contains 8 oxygen atoms, Th–O interatomic distance being 2.37 Å (Table 3). This suggests that Th has the same immediate environment in muratiate-based ceramics as in ThO_2, *i.e.* Th atom is situated in the center of a cube with 8 oxygen atoms in the corners (D_{4h} symmetry group), which agrees with the XPS data.[8] The modeling of the second coordination sphere suggested that it does not include Th atoms since the peak at ~3 Å observed in the graph of the radial structural function for the ceramics [Figure 3(*d*)] is absent in the ThO_2 graph [Figure 3(*b*)]. The best agreement between the

Table 2 Local structure of ThO_2 film (ΔE_0 = 5.51 ± 1.16 eV, R_f = 0.0006).[a]

No.	Element	*N*	*r*/Å	σ^2/Å^2
1	O	8	2.41 ± 0.01	0.005 ± 0.001
2	Th	12	3.98 ± 0.01	0.005 ± 0.001
3	O	24	4.65 ± 0.02	0.004 ± 0.002

[a] No. is the number of sphere, *N* is the number of atoms, *r* is the distance from Th to atoms of the coordination sphere, σ^2 is the Debye–Waller factor, ΔE_0 is the change in the absorption edge, R_f is the *R*-factor. Intervals: *k* = 2–10 Å^{-1}, *R* = 1.5–4.6 Å.

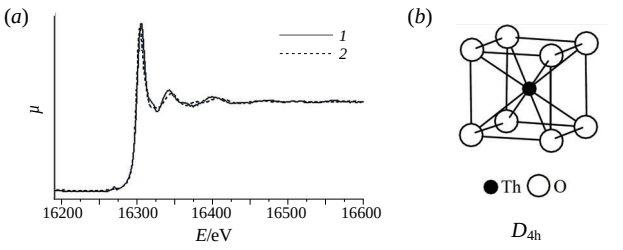

Figure 2 (*a*) Normalized Th L_{III} XAS spectra of (*1*) ThO_2 film and (*2*) muratiate-based ceramics; (*b*) structure of the immediate environment of Th^{4+} in ThO_2.

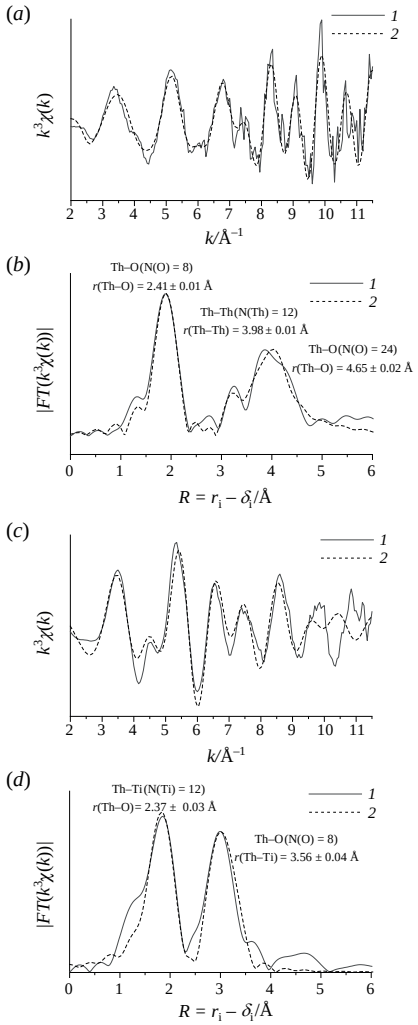

Figure 3 The EXAFS spectra at Th L_{III}-edge of (*a*) ThO_2 crystal film and (*c*) muratiate ceramics under the assumption that the second coordination sphere is formed by 12 atoms of Ti with (*b*), (*d*) their respective Fourier transforms moduli: (*1*) experimental and (*2*) best-fit model data; r_i is the interatomic distance; σ_i is the linear by *k* part of the phase shift, where *k* is the wave vector.

Table 3 Quantitative calculation results of the local atomic structure of models with different atoms in the second coordination sphere of thorium.[a]

Element in the 2nd coordination sphere	No.	Element	*N*	*r*/Å	σ^2/Å^2	ΔE_0/eV	R_f
Ti	1	O	8	2.37 ± 0.03	0.010 ± 0.004	2.51 ± 3,46	0.008
	2	Ti	12	3.56 ± 0.04	0.014 ± 0.003		
Fe	1	O	8	2.37 ± 0.02	0.010 ± 0.002	0.52 ± 2.66	0.004
	2	Fe	12	3.50 ± 0.03	0.016 ± 0.002		
Mn	1	O	8	2.37 ± 0.02	0.010 ± 0.003	1.11 ± 2.93	0.004
	2	Mn	12	3.51 ± 0.03	0.016 ± 0.002		
Ca	1	O	8	2.37 ± 0.04	0.009 ± 0.004	1.95 ± 3.70	0.014
	2	Ca	12	3.59 ± 0.04	0.015 ± 0.004		
Al	1	O	8	2.32 ± 0.04	0.009 ± 0.004	–5.26 ± 3.36	0.034
	2	Al	12	3.70 ± 0.06	0.005 ± 0.004		
Zr	1	O	8	2.37 ± 0.05	0.008 ± 0.006	–0.05 ± 0.05	0.101
	2	Zr	12	3.84 ± 0.03	0.013 ± 0.004		

[a] No. is the sphere number, *N* is the number of atoms, *r* is the distance from thorium to atoms of the coordination sphere, σ^2 is the Debye–Waller factor, ΔE_0 is the change in the absorption edge, R_f is the *R*-factor. Intervals: *k* = 2–10 Å^{-1}, *R* = 1.5–3.4 Å were used in all cases.

model and the experimental data was reached when the second coordination sphere was formed by 12 Ti atoms [Figure 3(*c*),(*d*)]. This number of atoms agrees with the composition of the thorium

second coordination sphere in ThO_2, whose cells are included in murataite structure. In this case, the first peak corresponds to the coordination number of Th equal to 8 and r(Th–O)= 2.37 ± 0.03 Å (Table 3). This interatomic distance agrees with that in ThO_2 film (2.41 Å). The assumption that the second coordination sphere is formed by 12 titanium atoms gives the best agreement of ΔE_0 (Table 3) with that yielded by modeling of ThO_2 spectrum (Table 2). The substitution of titanium atoms with manganese or iron atoms provides a satisfactory agreement with the experimental data (Table 3). The assumption that the thorium second coordination sphere at ~3.5 Å is formed by Zr, Al and Ca in the ceramics worsens the agreement with the experimental data since the R-factor grows and ΔE_0 (Table 3) corresponds less with that found by modeling of ThO_2 spectrum (Table 2). Modeling of the second coordination sphere yields a worse agreement between the calculated and experimental spectra in the row (R_f in parentheses): Ti (0.008) ≈ Fe (0.004) ≈ Mn (0.004) < Ca (0.014) < Al (0.034) < Zr (0.101).

Thus, we have obtained EXAFS spectra of crystalline ThO_2 film and murataite ceramics (Al,Ca,Ti,Mn,Fe,Zr,Th)O_x. The compositions of the first three coordination spheres and interatomic distances to thorium were clarified. It was confirmed that Th^{4+} ion in ThO_2 is situated in the center of a cube formed by 8 oxygen atoms [r(Th–O) = 2.38 ± 0.03 Å]. The second coordination sphere of thorium [r(Th–M) ≈ 3.5 Å] in murataite ceramics is represented by 3d metals: titanium, iron or manganese. As a result, it was proven that thorium in murataite ceramics is in the most stable state.

S.N.K., A.L.T., V.G.P. acknowledge support by the Russian Ministry of Science and Higher Education (grant no. 075-15-2021-1353).

Online Supplementary Materials

Supplementary data associated with this article can be found in the online version at doi: 10.1016/j.mencom.2023.01.043.

References

1 M. B. Remizov, P. V. Kozlov, V. P. Borisenko, I. I. Dement'eva, P. A. Blokhin and A. A. Samoylov, *Radioaktivnye otkhody*, 2018, no. 3 (4), 102 (in Russian).
2 G. R. Lumpkin, in *Experimental and Theoretical Approaches to Actinide Chemistry*, 1st edn., eds. J. K. Gibson and W. A. de Jong, Wiley, 2018, pp. 333–377.
3 *Radioactive Waste Forms for the Future*, eds. W. Lutze and R. C. Ewing, Elsevier, Amsterdam, 1988.
4 *Handbook of Advanced Radioactive Waste Conditioning Technologies*, ed. M. I. Ojovan, Woodhead Publishing, Cambridge, 2011.
5 S. V. Stefanovsky and S. V. Yudintsev, *Russ. Chem. Rev.*, 2016, **85**, 962.
6 *The Chemistry of the Actinide and Transactinide Elements*, 4th edn., eds. L. R. Morss, N. M. Edelstein and J. Fuger, Springer, 2011.
7 M. S. Nickolsky and S. V. Yudintsev, *Crystallogr. Rep.*, 2021, **66**, 130.
8 K. I. Maslakov, Yu. A. Teterin, O. I. Stefanovskaya, S. N. Kalmykov, A. Yu. Teterin, K. E. Ivanov, S. V. Yudintsev and B. F. Myasoedov, *Radiochemistry*, 2020, **62**, 599 (*Radiokhimiya*, 2020, **62**, 402).
9 A. E. Putkov, K. I. Maslakov, A. Yu. Teterin, Yu. A. Teterin, M. V. Ryzhkov, K. E. Ivanov, S. N. Kalmykov and V. G. Petrov, *Radiochemistry*, 2022, **64**, 133 (*Radiokhimiya*, 2022, **64**, 133).
10 T. Yamashita, N. Nitani, T. Tsuji and H. Inagaki, *J. Nucl. Mater.*, 1997, **245**, 72.

Received: 14th July 2022; Com. 22/6959